Docking and Scoring With Target-Specific Pose Classifier Succeeds in Native-Like Pose Identification But Not Binding Affinity Prediction In The CSAR 2014 Benchmark Exercise

Supporting Information

Regina Politi^{1,2}, Marino Convertino², Konstantin Popov², Nikolay V. Dokholyan^{2*} and Alexander Tropsha^{1*}.

¹Laboratory for Molecular Modeling, Division of Chemical Biology and Medicinal Chemistry, UNC Eshelman School of Pharmacy, University of North Carolina at Chapel Hill, Chapel Hill, NC, 27599, USA.

* Corresponding Authors:

Dr. Nikolay V. Dokholyan, Biochemistry and Biophysics Department, University of North Carolina, 120 Mason Farm Road, CB #7260 Genetic Medicine, Chapel Hill, NC, 27599, USA. Phone: +1 919 843-2513. E-mail: dokh@unc.edu;

Dr. Alexander Tropsha, Division of Chemical Biology and Medicinal Chemistry, UNC Eshelman School of Pharmacy, University of North Carolina, 301 Pharmacy Lane, Chapel Hill, NC, 27599, USA. Phone +1 919 966-2955. E-mail: alex_tropsha@unc.edu.

²Department of Biochemistry and Biophysics, School of Medicine, University of North Carolina at Chapel Hill, Chapel Hill, NC, 27599, USA.

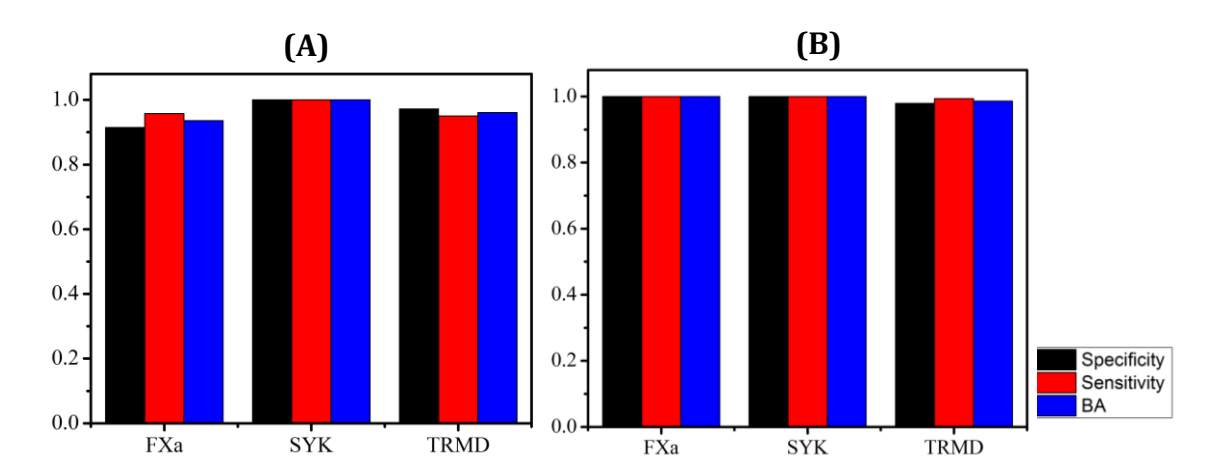


Figure S1. Statistical parameters obtained for the native/decoy classification models (poses are discriminated using a threshold of RMSD = 2Å) for three CSAR targets. External prediction performances (sensitivity, specificity, and BA) estimated according to a 5-fold external cross validation procedure. (A) shows statistical parameters for PDB structures used in Phase 1 and (B) shows statistical parameters for PDB structures used in Phase 2.

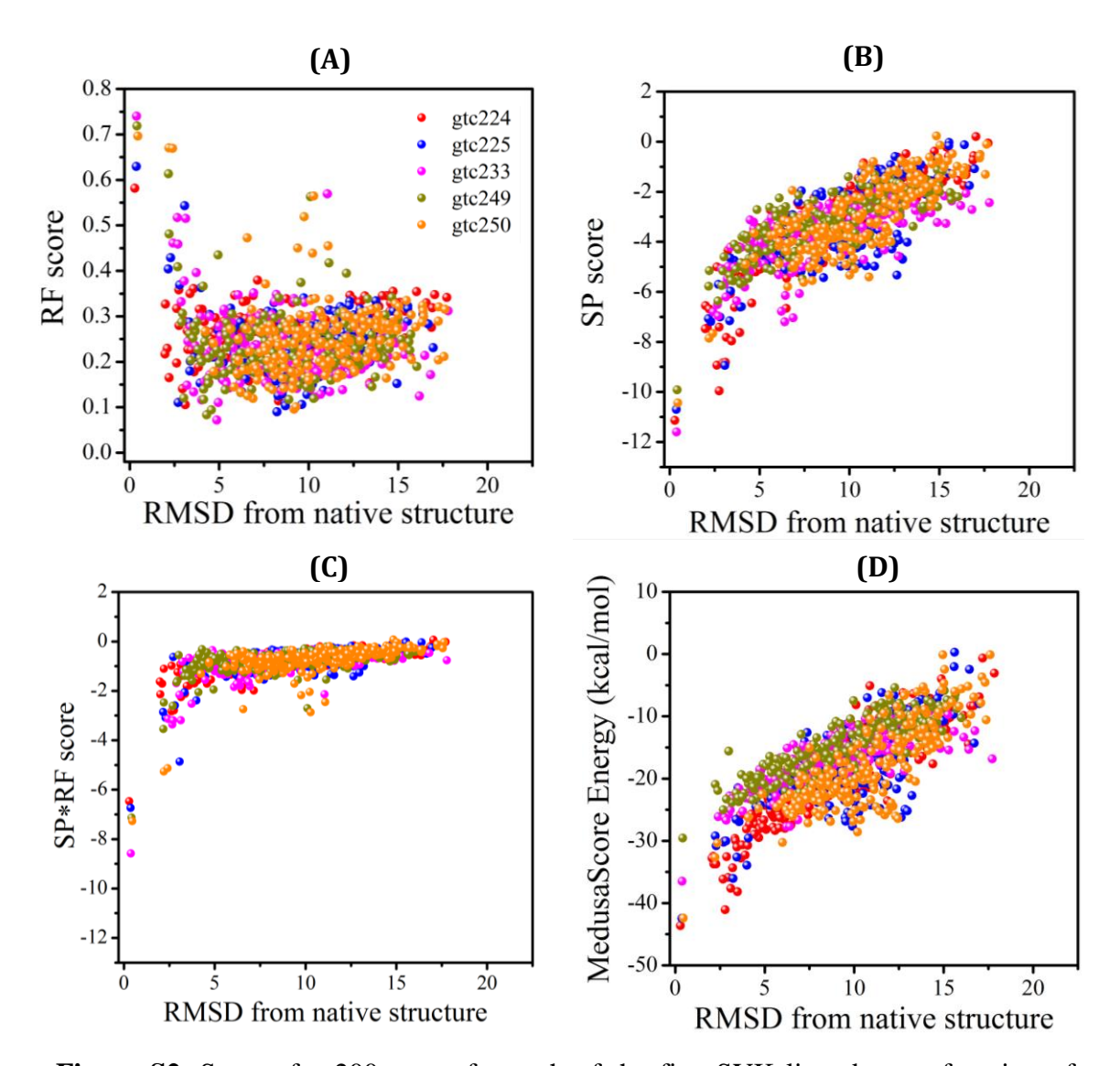


Figure S2. Scores for 200 poses for each of the five SYK ligands as a function of RMSD: (A) RF scores; (B) Glide SP docking scores; (C) Product of Glide SP and RF scores; (D) MedusaScore docking energies.

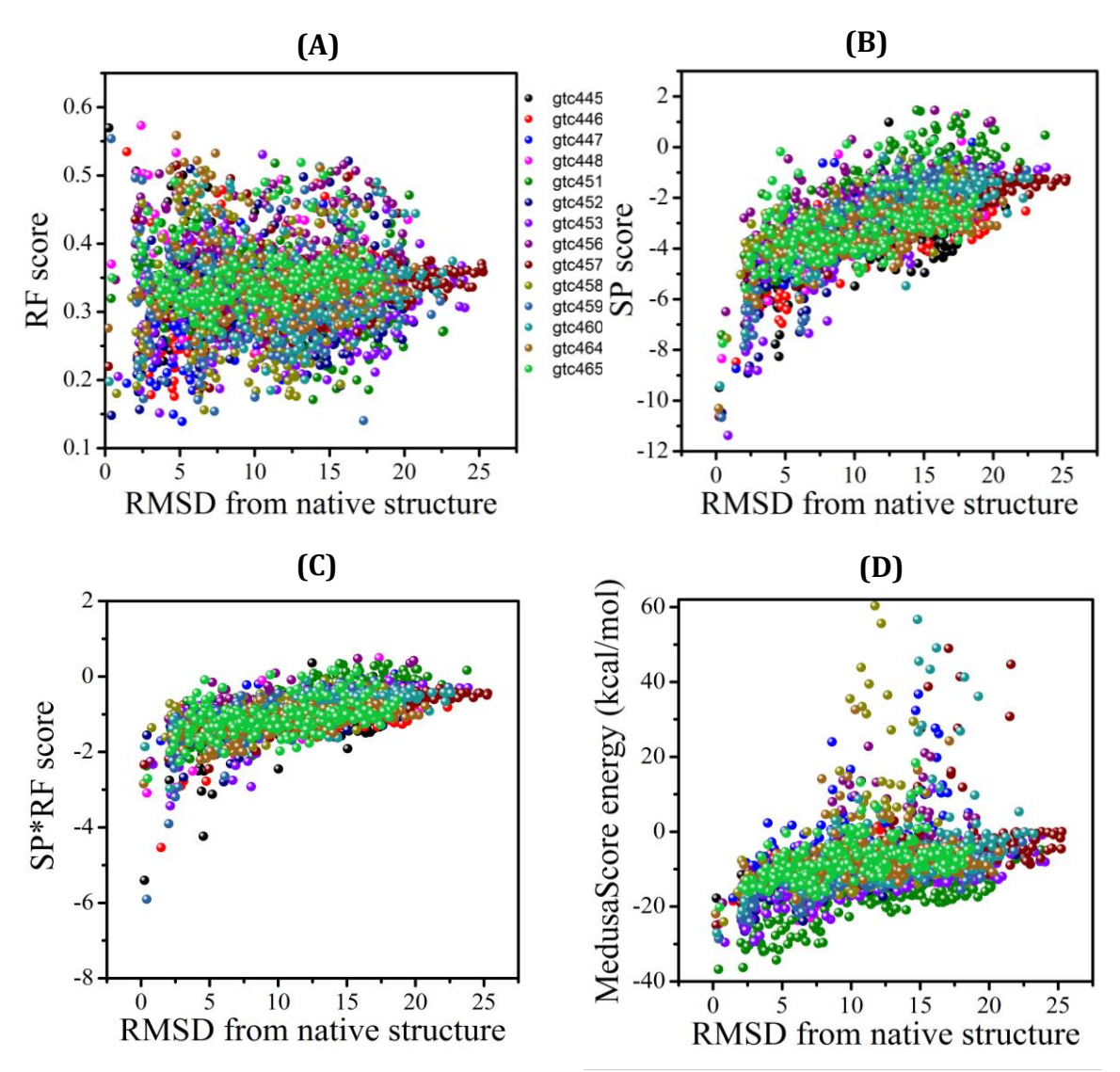


Figure S3. Scores for 200 poses for each of the 14 TRMD ligands as a function of RMSD: (A) RF scores; (B) Glide SP docking scores; (C) Product of Glide SP and RF scores; (D) MedusaScore docking energies.

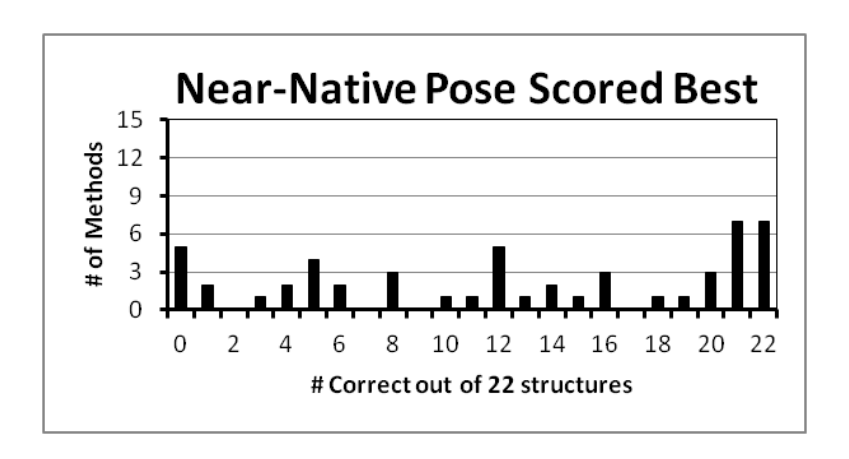


Figure S4. Summary for the results of Phase 1 provided by the organizers. Of the 52 methods submitted 7 scored all 22 complexes correctly, identifying each native-like pose with the top score.

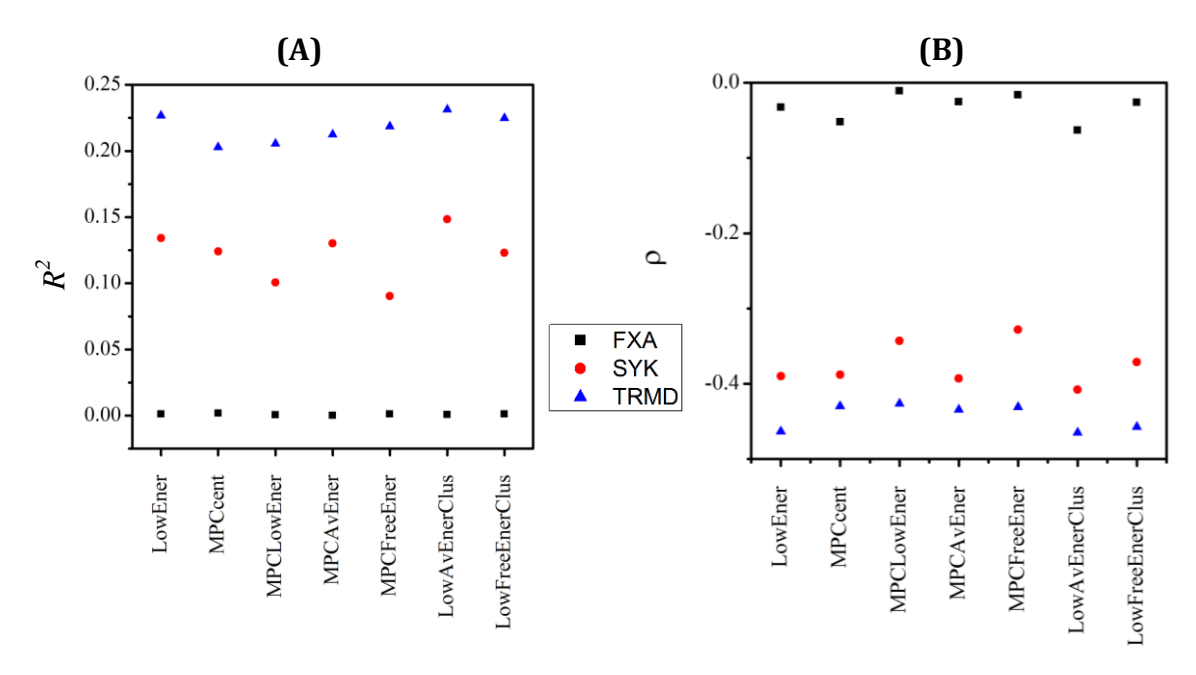


Figure S5. Prediction accuracy as a result of different clustering methods: (A) Measured as squared Pearson correlation (R^2) . (B) Measured as Spearman correlation (ρ) .

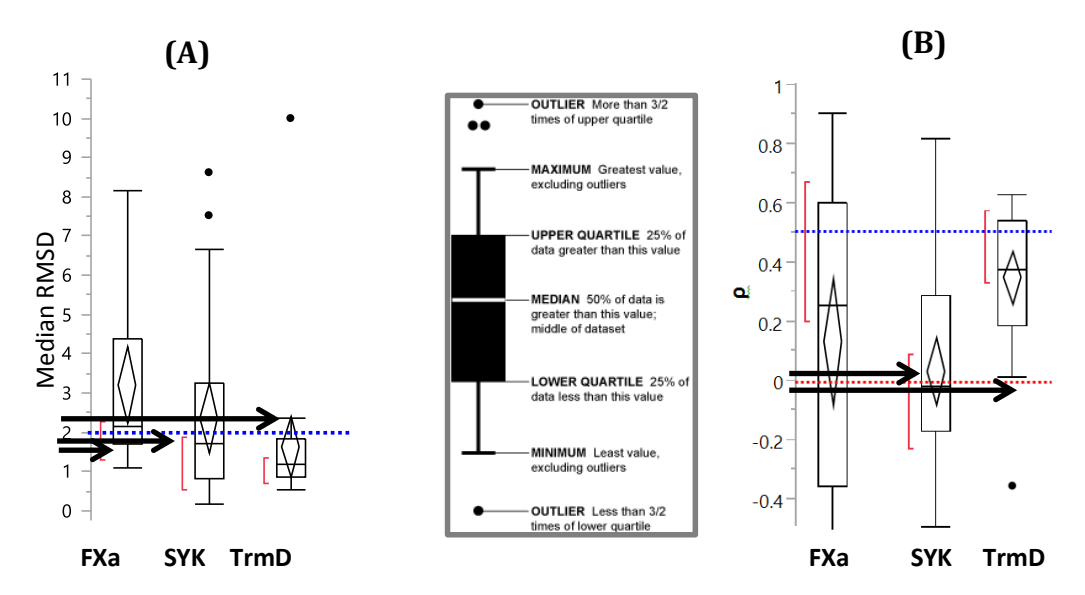


Figure S6. Summary for the results of Phase 2 provided by the organizers only for the ligands that have crystal structures available (5 for FXa, 9 for SYK, and 31 for TrmD): (A) Distribution of Median RMSDs (top pose) from each method out of 35 methods submitted. Black arrows show median RMSD achieved by our group for these particular ligands (1.56 for FXa, 1.76 for SYK and 2.35 for TRMD). (B) Spearman correlation (ρ) for the same ligands used in RMSD calculations. Black arrows show results of our group (-1 for FXa, 0.025 for SYK and -0.04 for TRMD). Blue dashed lines mark the definition of "good performance" for this study: RMSD \leq 2 Å and $\rho \geq$ 0.5. The red dashed line differentiates between positive and negative correlations to experiment. The red bar indicates the shortest interval that contains 50% of the data.

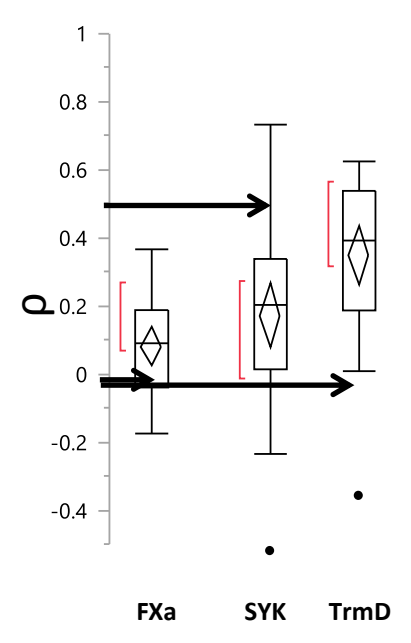


Figure S7. Spearman correlation (ρ) provided by the organizers for <u>all</u> the ligands in Phase 2: The ρ are given for the entire set of ligands provided to participants (163 for FXa, 276 for SYK, and 31 for TRMD). The red bar indicates the shortest interval that contains 50% of the data. Black arrows show results submitted by our group (-0.038 for FXa, 0.049 for SYK and -0.04 for TRMD).

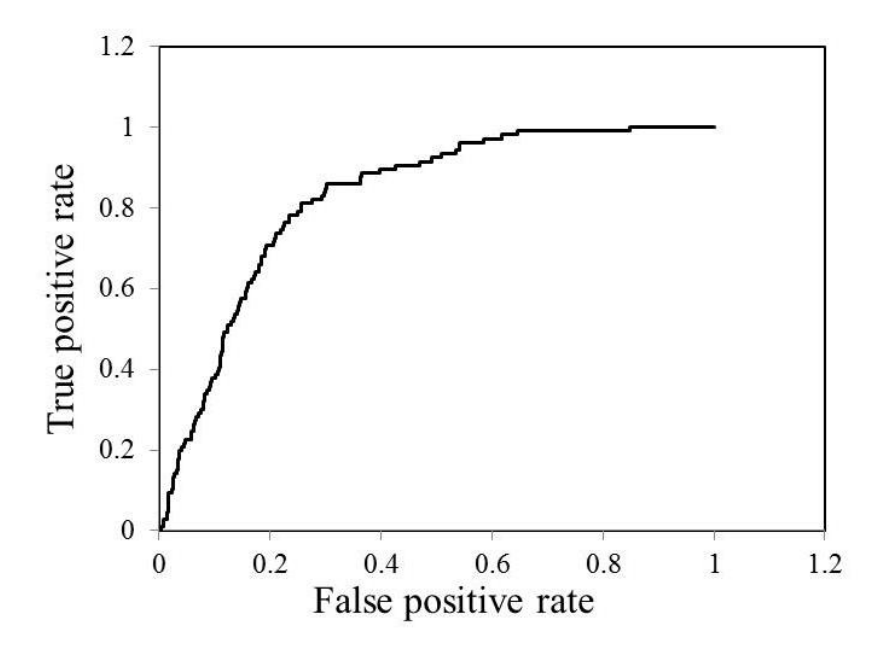


Figure S8. Receiver Operating Characteristic (ROC) plot for recovering FXa ligands by virtual screening of the DUDE benchmarking database. Solid line corresponds to FXa ligands provided by the CSAR organizers.

.